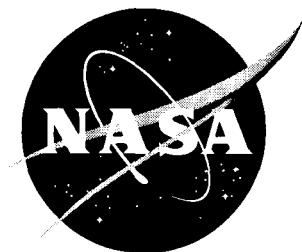# An Analysis of Measured Pressure Signatures From Two Theory-Validation Low-Boom Models

Robert J. Mack
Langley Research Center, Hampton, Virginia

Since its founding, NASA has been dedicated to the advancement of aeronautics and space science. The NASA Scientific and Technical Information (STI) Program Office plays a key part in helping NASA maintain this important role.

The NASA STI Program Office is operated by Langley Research Center, the lead center for NASA's scientific and technical information. The NASA STI Program Office provides access to the NASA STI Database, the largest collection of aeronautical and space science STI in the world. The Program Office is also NASA's institutional mechanism for disseminating the results of its research and development activities. These results are published by NASA in the NASA STI Report Series, which includes the following report types:

- TECHNICAL PUBLICATION. Reports of completed research or a major significant phase of research that present the results of NASA programs and include extensive data or theoretical analysis. Includes compilations of significant scientific and technical data and information deemed to be of continuing reference value. NASA counterpart of peer-reviewed formal professional papers, but having less stringent limitations on manuscript length and extent of graphic presentations.

- TECHNICAL MEMORANDUM. Scientific and technical findings that are preliminary or of specialized interest, e.g., quick release reports, working papers, and bibliographies that contain minimal annotation. Does not contain extensive analysis.

- CONTRACTOR REPORT. Scientific and technical findings by NASA-sponsored contractors and grantees.

- CONFERENCE PUBLICATION. Collected papers from scientific and technical conferences, symposia, seminars, or other meetings sponsored or co-sponsored by NASA.

- SPECIAL PUBLICATION. Scientific, technical, or historical information from NASA programs, projects, and missions, often concerned with subjects having substantial public interest.

- TECHNICAL TRANSLATION. English-language translations of foreign scientific and technical material pertinent to NASA's mission.

Specialized services that complement the STI Program Office's diverse offerings include creating custom thesauri, building customized databases, organizing and publishing research results ... even providing videos.

For more information about the NASA STI Program Office, see the following:

- Access the NASA STI Program Home Page at *http://www.sti.nasa.gov*

- E-mail your question via the Internet to help@sti.nasa.gov

- Fax your question to the NASA STI Help Desk at (301) 621-0134

- Phone the NASA STI Help Desk at (301) 621-0390

- Write to:
  NASA STI Help Desk
  NASA Center for AeroSpace Information
  7121 Standard Drive
  Hanover, MD 21076-1320

NASA/TM-2003-212423
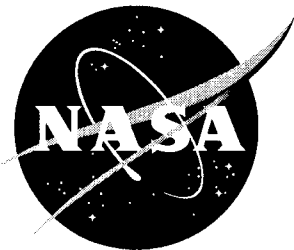
An Analysis of Measured Pressure Signatures From Two Theory-Validation Low-Boom Models

Robert J. Mack
Langley Research Center, Hampton, Virginia

October 2003

Available from:

Summary

Two wing/fuselage/nacelle/fin concepts were designed using the sonic-boom minimization theory, the sonic-boom analysis methods, and the low-boom design methodology developed by the late 1980's. This effort was made to check the validity and applicability of the latest sonic-boom design and analysis methods. Models of these concepts were built, and their pressure signatures were measured in the wind-tunnel. In this report, an analysis of these measured pressure signatures is presented and discussed. An analysis of the results of this test lead to three conclusions: (1) the existing methodology could adequately predict sonic-boom characteristics of wing/fuselage/fin(s) configurations if the equivalent area distributions of each component were smooth and continuous; (2) this methodology needed revision so the flow-field effects of engine-nacelle volume and the nacelle-wing interference lift disturbances could be accurately predicted; and (3) current nacelle-configuration integration methods had to be modified. With these changes implemented, the existing sonic-boom reduction or minimization methods could be effectively applied to supersonic-cruise concepts so they would generate acceptable/tolerable sonic-boom overpressures during cruise.

Introduction

By the close of the Supersonic Cruise Aircraft Research (SCAR) Program, considerable advancements had been made in the development of methods for low-boom design and sonic-boom analysis. These methods were based primarily on the sonic-boom propagation theories of Whitham and Walkden, along with the theoretical and experimental contributions from dozens of engineers and scientists. Whitham introduced a first-order method, reference 1, for predicting the far-field shock system generated by a body of revolution traveling at supersonic speed. Walkden extended the applicability of Whitham's method to lifting wing/bodies by showing that in the far field, sonic boom disturbances from a lifting wing/body could be predicted as though they were generated by a body of revolution, reference 2. These two basic contributions made it possible to predict most of the sonic-boom characteristics of real aircraft in supersonic-cruise flight.

L. B. Jones, reference 3, introduced a theory for minimizing the sonic-boom generated by a body of revolution which depended on localized nose blunting. The application of his theory reduced the far-field N-wave nose and tail shocks by minimizing the impulse (area under the positive section of the overpressure). Seebass and George, reference 4, extended Jones' low-boom minimization so supersonic-cruise vehicles could generate shaped rather than N-wave minimum shock pressure signatures. They showed that these shaped pressure signatures could reduce the nose and tail shock strengths significantly even though some wave drag penalties were still present. Darden, reference 5, changed the Seebass and George F-function nose-blunting from a delta-function to a slender triangular "spike", and suggested that the wave drag of a wing-body configuration could be reduced with only a small increase in pressure signature shock strength.

McLean, reference 6, addressed the question of how far below the aircraft the near-field pressure signature shape might persist through the atmosphere. He concluded that during the supersonic climb/acceleration segment of the mission, the aircraft's pressure signature might retain many of its near-field non-N-wave characteristics if the configuration's volume and lift distributions were appropriately tailored.

Carlson et. al. extended McLean's results further by incorporating low-boom technology into the

designs of some Supersonic Transport (SST) concepts, reference 7. He demonstrated that reductions were possible in the sonic boom generated during supersonic cruise. Similar studies, references 8 to 18, carried out concurrently with these minimization efforts, also showed that Whitham theory was capable of accurately predicting pressure signatures at mid-field as well as far-field distances. Under the impetus of these developments, the scope of sonic-boom theory and wind-tunnel-experiment studies moved from the far-field toward the near-field. Wind-tunnel models used in these new studies were larger and more complex, so it became possible to incorporate more accuracy and sophistication in the their components. Results from studies with these larger models, references 9, 10, 13 and 15, demonstrated that, when judiciously-applied, Whitham-Walkden theory had useful prediction capabilities at low supersonic Mach numbers if the conceptual aircraft and their models were sufficiently thin and slender.

Based on the successful results from this body of experimental data, five 1:600 scale wing-fuselage wind-tunnel models, reference 19, were designed with boom-minimization methodology applied to the combined volume and lift contributions. Two of these models were reference wing-body models, 4 to 5 inches in length, while the other three, 6 inches in length, had wing-planforms and fuselages shaped for minimum sonic boom at Mach numbers of 1.50 and 2.70 . To keep design variables to a minimum, these configurations had no nacelles, fins, wing camber and twist, or fuselage camber. Their measured pressure signatures showed that at Mach 1.5, theory and experiment agreed reasonably well. However, at Mach 2.7, this good agreement was found only along the forward half of the model's measured pressure signatures. In the subsequent analysis of the data, it was determined that part of this disagreement was caused by a linearized-theory method used for predicting the lift equivalent-area distributions. This need for a better wing-analysis and performance-prediction method led to the development of a modified-linearized-theory wing analysis code, reference 20 during the years following the wing-body model wind-tunnel tests. Since wing lift contributed significantly to sonic-boom noise, the addition of this improved wing analysis code to the existing array of design and analysis codes increased the possibilities that credible low-sonic-boom SST concepts could be designed, and that accurate predictions of complete ground pressure signatures could be made.

Although high-speed civil transport technology and sonic-boom research was gradually terminated between the late 1970's and early 1980's, defining and assessing the state of technology for solving the problems associated with commercial flight at supersonic cruise continued. Then, during the latter part of the 1980's, technical interest in high-speed civil transports was revitalized. Existing sonic-boom methods for design and analysis were evaluated with the intent of become reacquainted with existing methodology. New models were designed and built to determine which techniques and methods would accurately predict the ground-level sonic boom disturbances generated by the proposed conceptual supersonic-cruise aircraft.

In this report, measured pressure signatures generated by two wind-tunnel models of conceptual supersonic-cruise aircraft are presented and analyzed. Their configuration geometries, reference 21, were designed and tailored to assess the full capabilities of existing sonic-boom design methods, sonic-boom analysis methods, and low-boom minimization methods in use at the end of the 1980's. These wind-tunnel models, built at a scale of 1:300, were about 12 inches in length; large enough that the engine flow-field disturbances could be simulated by ducted nacelles. Conclusions from an analyses of the test data were used to assess the capabilities of the existing design, analysis, and minimization methodology and to suggest modifications where required. Since the two concepts and their design methodology could strongly influence the configuration geometries of subsequent low-boom supersonic-cruise concepts, full confidence in these design, analysis, and minimization methods was necessary.

2

Nomenclature

b wing span, ft

C_L lift coefficient

h cruise altitude, ft; or separation distance, in

M Mach number

p ambient pressure, psf

Δp incremental free-stream pressure, psf

S wing area, ft^2

x distance in the longitudinal direction, ft

Concept Design and Pressure-Signature Analysis

Conceptual supersonic-cruise aircraft were designed with methods developed during the Supersonic Cruise Aircraft Transport (SCAT) program of the 1960's to the 1980's. Using these methods, equivalent areas were computed from the volume and lift contributions and then summed for the calculation of concept F-functions. Following these steps, the F-functions were used to predict ground pressure signatures. Sources of the volume contributions were the fuselage, the wing, the canard and/or horizontal tail, the fin, and the engine nacelles. Lift contributions came from the wing and the nacelle-wing interference lift. The equivalent areas of all components were assumed to be smooth and continuous. Curved wing leading edges, blended wing-fuselage junction, and subsonic wing and fin leading edges were features that met the continuous-area-growth criteria readily. Nacelles with inlets having very small lip angles, and small nacelle-wing interference-lift contributions were also believed to meet the smooth-area continuity criteria.

Two aircraft concepts were designed in this theory-validation study. One concept had a design Mach number of 2.0 with a "flat top" along the positive-pressure section of the ground pressure signature. The other had a design Mach number of 3.0, and the positive-pressure section of its pressure signature had a "ramp" shape. Each concept was similar to those in a previous set, reference 19, in that it was a wing/fuselage configuration. They were different in that each of them had four engine nacelles under the wing, and a vertical fin on the aft fuselage. Nacelles were simulated by a body of revolution with a central constant-area duct. The wing of each model had a mild camber and twist distribution, and the leading edges were curved with the leading-edge sweep changing smoothly from root to tip. Dihedral was added to the wing so the effective and the total lifting length would stay about the same at cruise angle of attack. The fuselage center line was cambered to match the camber line of the wing root chord. Concept design merits were determined by comparison of ground pressure signatures predicted with methods and codes described in references 22 and 23 with ideal pressure signatures derived from equations given in references 4 and 5. In the following sections, each low-boom concept and model is discussed, and the data obtained from the model is presented and analyzed.

The Mach 2 Concept

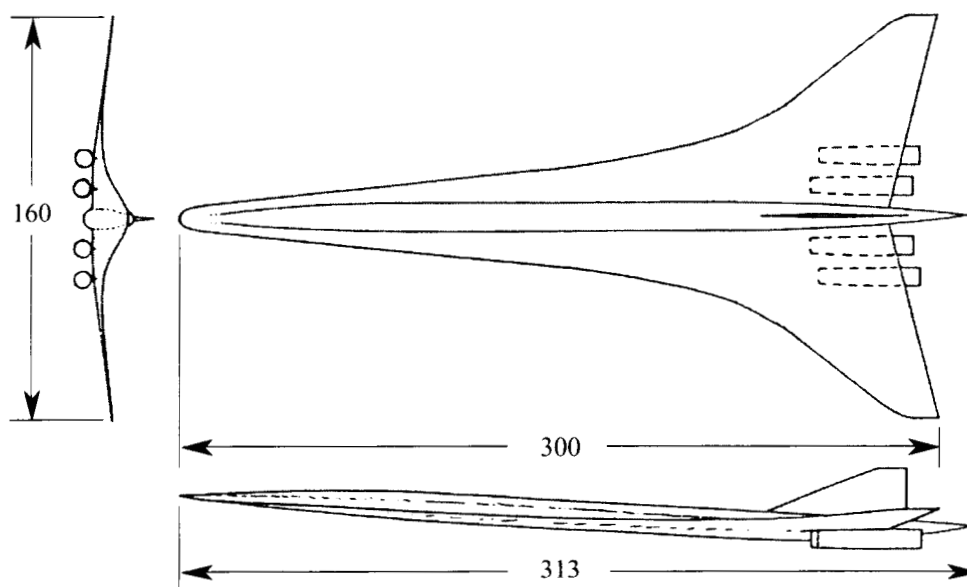A three view of the Mach 2 theory-validation concept is shown in figure 1.

Figure 1. Three view of the Mach 2 theory-validation concept.

In Appendix A, characteristic dimensions and the low-boom mission specifications of the Mach 2 theory-validation concept are listed. A numerical description of its geometry, in supersonic wave drag program format, reference 24, is presented in Appendix B.

The wind-tunnel model of the concept was 12 inches in length, and had an integral sting/balance which extended from the aft fuselage, well behind the trailing edge of the wing. The wing leading edge began with a sharply-rounded apex which smoothly blended into a long, highly-swept strake. This strake gradually reduced in sweep, and merged with the outer wing panels which also had subsonic leading edges. Engine nacelles were mounted two to a side under the wing trailing edge. Two sets of nacelles were built for the Mach 2 model. One set was made from composite materials and had rounded and blunt inlet lips, while the other set was metal with sharp-edged inlet lips; a set shaped more like real engine nacelles. Pressure signatures, like that seen in figure 2, were measured from the model with sharp inlet lip metal nacelles.
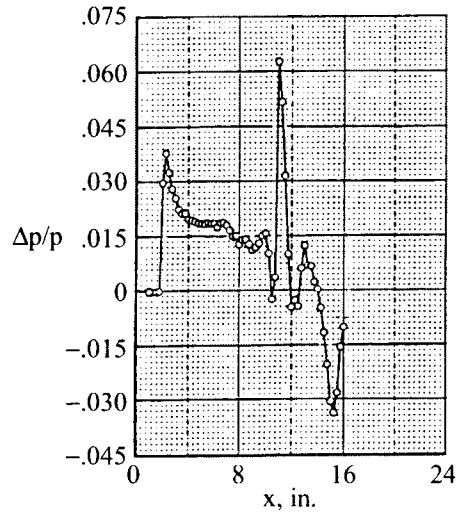
Figure 2. Pressure signature from the Mach 2 model with sharp-lip metal nacelles. M = 2.0, h = 6 inches, and model was at cruise C_L.

Since the four nacelles had finite-sized inlet-lip angles and generated nacelle-wing interference lift, they were thought to be the cause of the sharp pressure spike seen aft of the nose shock. This hypothesis was verified by measuring a pressure signature, figure 3, with the nacelles off the model.
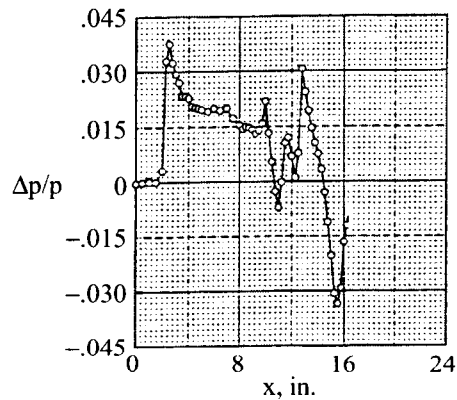

Figure 3. Pressure signature from the Mach 2 model without nacelles. M = 2.0, h = 6 inches, and model was at cruise C_L.

Shocks are still seen aft of the nose shock and ahead of the expansion preceding the tail shock, but they are smaller and located in the region where the nacelles had been mounted. As the distance between model and survey probe increased, these disturbances attenuated, as seen in figure 4.
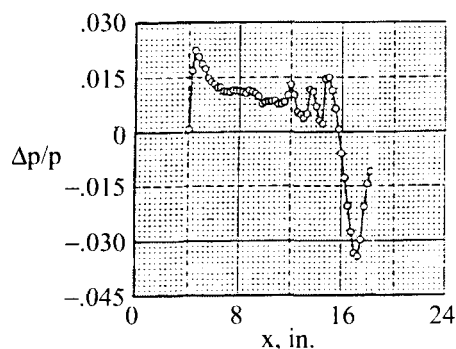
.030

.015

0

$\Delta p/p$

−.015

−.030

−.045

0   8   16   24

x, in.

Figure 4. Pressure signature from the Mach 2 model without nacelles. M = 2.0, h = 12 inches, and model was at cruise C_L.

Two interesting features were noted on this near-field pressure signature. First, the shocks behind the nose shock and ahead of the expansion have noticeably attenuated with the attenuation of the in-between disturbances more noticeable than that of the nose shock. Second, these disturbances have remained stationary relative to the nose shock as the measurement distance increased from 6 to 12 inches. If an averaging line were drawn through the pressure points in figures 2 to 4, ignoring for a moment the prominent nacelle shock in figure 2, pressure signatures with almost "flat tops" would be seen with the mean pressure line lower in figure 4 than in figures 2 and 3. This suggested that the existing low-boom design method was applicable to components with smoothly-continuous equivalent areas. However, the ducted nacelles on the concept and model violated this criteria. This suggested that new methods needed to be developed so that nacelles could be properly integrated with other components and low boom overpressure constraints could be achieved.

These pressure-signature shape trends were also seen in figure 5, on one of three pressure signatures measured in an Ames Research Center facility. The pressure signature at a C_L about 5.9 percent higher than cruise C_L is shown because it was the closest to the design condition.
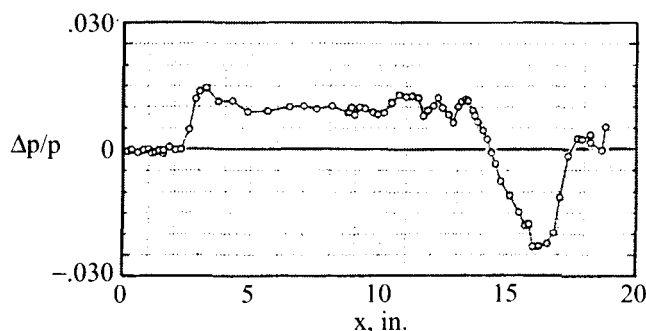
.030

$\Delta p/p$ 0

−.030

0   5   10   15   20

x, in.

Figure 5. Pressure signature from the Mach 2 model without nacelles[1]. M = 2.0, h = 28 inches, and model was at C_L = 0.072 (5.9 percent higher than the cruise C_L).

Note that the top of the pressure signature in figure 5 has become flatter as the separation distance has increased even though the model is carrying more lift than at cruise. Moreover, the pressure disturbances just ahead of the expansion to the tail shock have attenuated to where they are barely noticeable above the average positive overpressures. Thus, the shape along the positive pressure length of the signature is more

---

[1] Pressure signature data courtesy of Joel Mendoza and Raymond Hicks of the Ames Research Center.

nearly the "flat-top" intended in the design process. This observation reinforced the conclusion that low-boom design and analysis methods were applicable to supersonic-cruise vehicles. However, there was still a need for new nacelle integration methods.

There were no pressure signatures measured at a separation distance of 28 inches from the Mach 2 wind-tunnel model with sharp-lip metal nacelles, but there was one measured at this distance, figure 6, from the model with nacelles made of composite material.
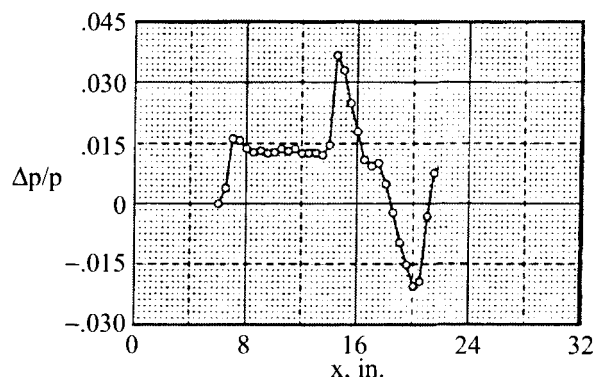

Figure 6. Pressure signature from the Mach 2 model with composite nacelles. M = 2.0, h = 28 inches, and model was at cruise C_L.

The signature in figure 6 is simpler in shape than the signature in figure 2 due to attenuation. As before, a prominent nacelle-induced shock is seen between the nose shock and the tail expansion, with the nacelle-induced shock about the same as the nose-shock in both figures. The nacelle-inlet shocks were probably attached to the inlet lips of the metal nacelles because their lip angle was only about 3 degrees; a prediction in accordance with constant-area duct theory which predicted no choking in the flow through these nacelles. With the composite material nacelles, the inlet shocks were detached because the inlet lips were rounded and blunt, and the internal diameter was reduced in order to maintain the external shape and size of the nacelles. However, both types of wind-tunnel-model nacelles, one with sharp inlet lips and ones with blunt inlet lips, would have generated the strong shocks readily observed on measured pressure signatures.

For these reasons, it was concluded that these unforeseen disturbances on the desired flat-top pressure signatures were caused by nacelle volume and interference-lift effects. Nacelle-inlet lip shocks plus those reflected from the lower surface of the wing probably contributed at least half the strength of the observed shock strength; the growth of nacelle-wing interference lift on the lower surface of the wing probably caused the other half. All of these individual disturbances coalesced to form the large shocks observed in figures 2 and 6. Their presence emphasized the importance of using appropriate nacelle modeling and disturbance-theory methods in the evaluation of the nacelle's contribution to sonic boom, and also demonstrated the need for careful nacelle integration to achieve both high aerodynamic efficiency and low sonic boom.

The Mach 3 Concept

Except for the design Mach number and a pointed cusp-like nose instead of a distinctive "platypus" nose, the Mach 3 theory-validation concept and its corresponding wind-tunnel model strongly resembled the Mach 2 concept and wind-tunnel model. This specially shaped nose was a feature introduced by the F-function modification, reference 5, to the sonic-boom minimization theory described in reference 4. It

permitted design flexibility in the trade between sonic-boom shock strength and wave drag penalties on a supersonic-cruise aircraft concept.

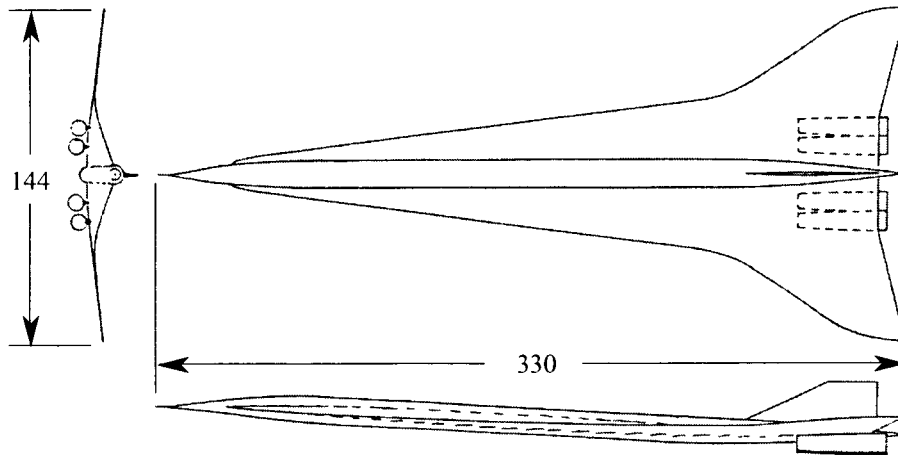A three view of the preliminary design of the Mach 3 concept is shown in figure 7.

Figure 7. Three view of the initial Mach 3 theory-validation concept.

Characteristic dimensions and some low-boom mission specifications of the Mach 3 concept are listed in Appendix A. Like the Mach 2 concept, the wing area on the initial Mach 3 concept was not limited by aerodynamic efficiency, but was sized and shaped to meet low-boom constraints. Later, it was reduced by 10 percent so it was closer to the area on the Mach 2 concept. A numerical description of the resized Mach 3 concept, used to design the wind-tunnel model, is given in Appendix C. A three view of this resized Mach 3 concept is shown in figure 8.
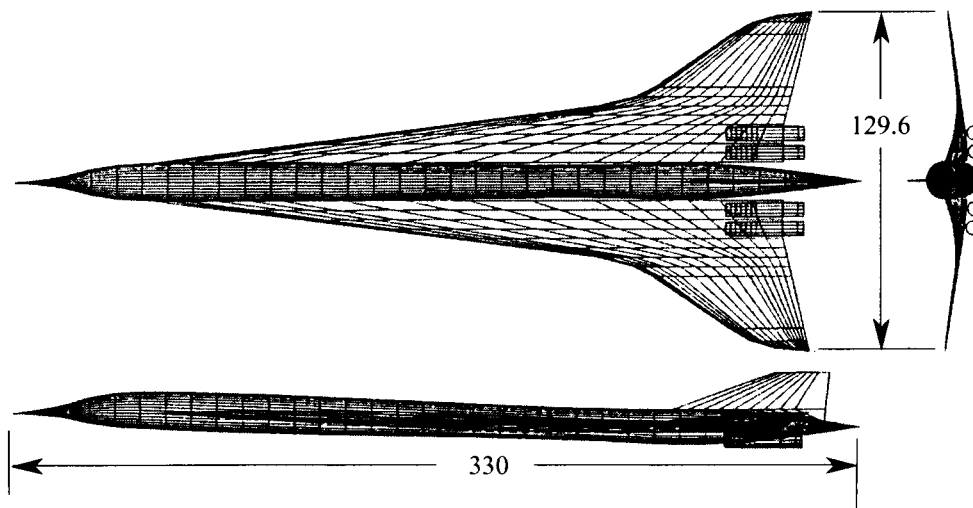

Figure 8. Three view of the resized Mach 3 theory-validation concept.

The wind-tunnel model of the resized Mach 3 concept was similar to the wind-tunnel model of the Mach 2 concept. Both had a sting/balance integrated with the aft end of the fuselage, well behind the wing trailing edge, and the wing/fuselage/nacelle/fin model was twelve inches in length with a cambered and twisted wing. The fuselage had a center line coincident with the wing root chord camber line, and four

ducted nacelles were mounted under the wing. Although the wing, fuselage, fin, and sting of the wind-tunnel model were made of stainless steel, the engine nacelles on this model were made of composite materials, like a set made for the Mach 2 model. However, after examining the pressure signatures from the Mach 3 model, which was tested first, a set of metal nacelles with sharp inlet lips was built for the Mach 2 model. Data from the Mach 2 model with the sharp-lipped metal nacelles was shown in figure 2, but there was no time to have a similar set made for the Mach 3 model. So, all of the Mach 3 pressure signatures were measured with and without the composite material nacelles.

A typical measured pressure signature generated by the Mach 3 model with the composite nacelles is shown in figure 9.
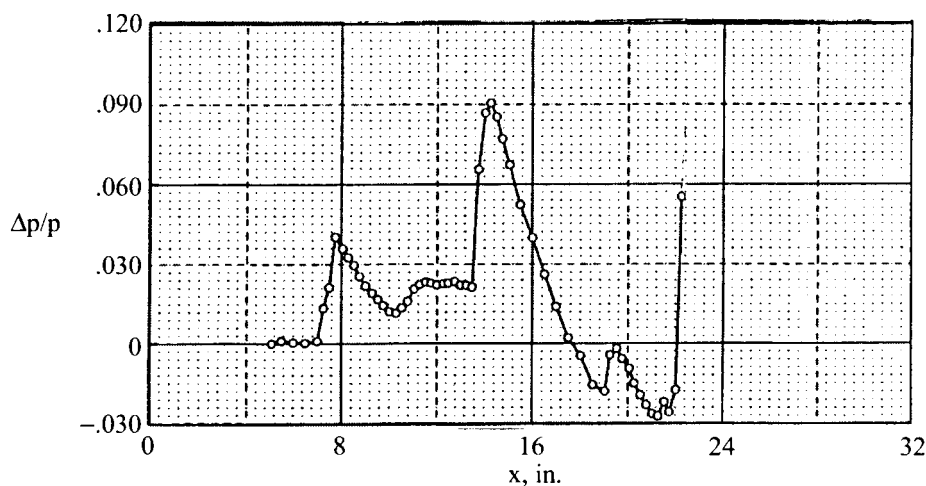

Figure 9. Pressure signature from the Mach 3 model with composite nacelles. $M = 2.96$, $h = 8.5$ inches, and model was at cruise C_L.

The pressure signature was measured at Mach 2.96, at the cruise C_L, and at a separation distance of about 8.5 inches. The narrow pressure spike following the nose shock on the pressure signature in figure 2 was seen in figure 9 as a broad, rounded, and strong pressure disturbance (shock) which lead directly into the pressure signature expansion, nacelle exhaust recompression, and tail shock. Like its counterpart on the Mach 2 model pressure signature, this large disturbance was produced by the combined volume and interference-lift effects from the four composite material engine nacelles. Some of the shock spreading was due to Mach number effects, some was due to the blunted lips on the nacelle inlets, and some by choked flow within the smaller internal duct. These last two effects were due to the use of composite materials rather than metal.

The large pressure jump at the tail was caused by the strain gauges mounted on the outside of the model sting. At a Mach number of 2, strain gauge shocks did not appear on the measured pressure signatures until well after the tail shock. However, at Mach 3, the strain gauge disturbances appeared much sooner along the pressure signature and partially encroached on the tail shock.

With the composite material nacelles off, the pressure signature in figure 10 was measured.
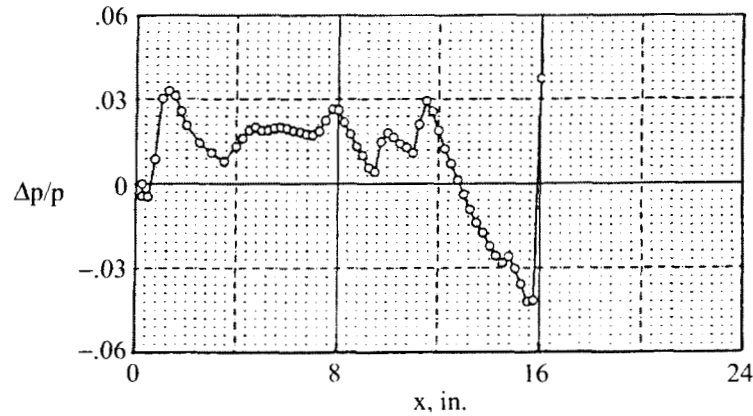
9

Figure 10. Pressure signature from the Mach 3 model without nacelles. M = 2.96, *h* = 8.5 inches, and model was at cruise C_L.

As was seen on the Mach 2 model pressure signature in figure 3, the strong pressure disturbance aft of the nose shock disappeared with the removal of the nacelles, leaving only small residual contributions from the wing-fuselage along the junction from leading to trailing edge. As seen on the pressure signature in figure 9, the unusually large pressure jump following the tail shock was due to the shocks off the strain gauges mounted on the outside of the model sting.

A second pressure signature at a Mach number of 2.96 was measured at a separation distance of 12 inches, and is presented in figure 11.
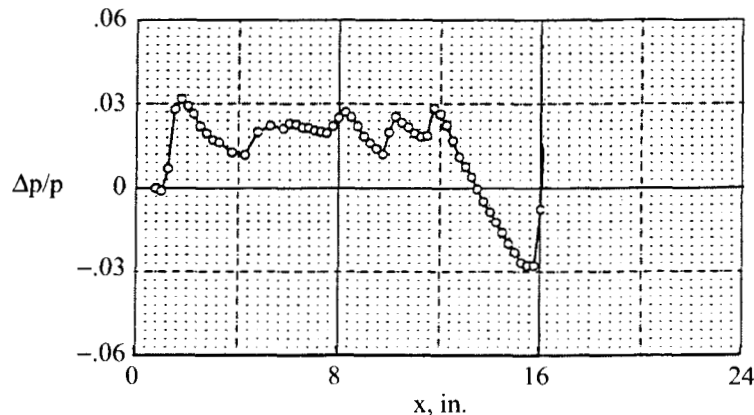

Figure 11. Pressure signature from the Mach 3 model without nacelles. M = 2.96, *h* = 12 inches, and model was at cruise C_L.

The changes in the forward part of the Mach 3 model pressure signatures seen in figures 10 and 11 are very similar to the corresponding changes observed on the Mach 2 model pressure signatures seen in figures 3 to 5. However, decreases in the magnitudes of the pressure peaks were smaller on the Mach 3 model pressure signatures because the model-survey probe separation distance increased from 8.5 to 12.0 inches rather than from 6.0 to 28.0 inches. There is no sign of a ramp in the measured pressures along the positive-pressure section of the signature in figure 11. Along the beginning of this section, disturbances come mainly from volume and only slightly from lift. Then, as the wing leading-edge sweep markedly changes, disturbances from lift appear more strongly. However, the cruise C_L was only 0.0442 instead of between 0.090 to 0.100, and the wing aspect ratio was 1.54 instead of about 2.0 usually seen on

10

supersonic-cruise concepts. So, the balance between volume and lift disturbances along the front of the positive-pressure section of the signature is tipped in favor of volume during these near-field measurements of pressure signatures. Volume disturbances attenuate more uniformly in radial directions than lift disturbances which are strongly vectored downward. This suggested, but did not definitely verify, that the minimization, analysis, and design methods employed to tailor the geometry of these concepts and models were as applicable at Mach 3 as they were at Mach 2. However, the area-rule planes were inclined at a shallower angle at Mach 3 than at Mach 2, so they influenced wing/fuselage volume and lift over longer lengths and made low-boom tailoring somewhat more difficult. Thus, without well-documented evidence of measured pressure signatures at separation distances larger than 12 inches and at cruise C_L values much higher than 0.0442, no strong conclusions can be made about the applicability of the low-boom minimization, design, and analysis methods Mach numbers as high as Mach 3.

Discussion

Comparisons of theoretical and measured pressure signatures could not be made because the methods used to design and tailor the configurations' geometry and analyze the concepts' sonic-boom characteristics were based on far-field theory, while the wind-tunnel pressure signatures were measured in the near-field. However, the shapes of these near-field pressure signatures were very similar to the shape of the individual models' Whitham F-functions calculated from an analysis of the volume and lift contributions of the model components. Used guardedly in this context, cautious interpretations had to be made of the near-field signatures results so that they could be useful in the evaluation of design methods and strategies. Also, the "aging", i.e. rate of change of the measured signatures' shape, shock strengths, and impulse with increasing distance, was observed and analyzed. Since pressure signatures "age" faster in the wind tunnel than in a stratified atmosphere, changes in signature shape with increasing distance were useful in judging the merits of a near-field effect hypothesis to explain the changes in the shape of the positive portion of the pressure signatures. Again, caution had to be used because of the near-field distances in the wind-tunnel tests.

The measured pressure signatures from the Mach 2 and the Mach 3 wind-tunnel models, with no nacelles, were very similar despite the difference in design Mach numbers. Low-boom tailoring of the nose and apex section of the wing generated, to a great extent, the desired pressure signature shape at both design Mach numbers. This part of the recorded data mirrored the results reported in reference 19.

The major difference between the results reported in reference 19 and these results was due to the ducted nacelles which were part of the design of the two concepts. There were, to be sure, problems in low-boom geometry tailoring associated with Mach number, but these were considered secondary in importance to the problems caused by the nacelle disturbances. Most of the past SST concepts, and all of the existing supersonic-cruise aircraft with capacities of 100 or more passengers, have been designed with engines positioned near the trailing edge of the wing. Only a few medium-sized subsonic passenger jets have engines located on the aft fuselage, although some supersonic-cruise business jet concepts had engines in this location. The measured pressure signatures in this study indicated that the engine nacelles mounted in the conventional under-the-wing location on the configurations contributed additional volume and interference-lift disturbances to the wing/fuselage/fin(s)-induced sonic-boom disturbances which had been held to desired low-boom levels, for the most part, by the application of Seebass and George minimization theory. Since difficulties in the low-boom tailoring of the wing/fuselage/fin(s) have been found to be aggravated by nacelle locations, new strategies for engine integration needed to be developed so that all configuration components could be harmoniously integrated to minimize, or at least reduce, sonic-boom noise on the ground.

Lift measured with strain gauges on the aft section of the sting to form a balance seemed to be a practical and workable idea if it were not for the strong shocks they created. This lift-measuring method could be used in the future if the strain gauges were submerged in grooves on the aft sting. By covering the strain gauges and their connection wiring with epoxy, and then smoothing their surfaces, the sting's smooth exterior contours could be preserved.

Concluding Remarks

Wind-tunnel measurements were made of pressure signatures generated by two models of concepts designed with existing 1960's to 1980's methodology for predicting sonic-boom characteristics of supersonic-cruise aircraft, as well as for designing conceptual aircraft with low-sonic-boom characteristics. Results from an analysis of these pressure signatures were used to evaluate and/or validate the capabilities of the design codes, the analysis codes, and the methodology. Four conclusions were made on the basis of these results:

(1) existing methodology could adequately predict sonic-boom characteristics of wing/fuselage/ fin(s) configurations if their individual components' equivalent area distributions were smooth and continuous;

(2) minimization theories and methods were capable of guiding the design of the forward sections of low-boom concepts and tailoring the equivalent areas of concept components as long as these equivalent areas were smooth and continuous;

(3) conventional sonic-boom analysis methods for predicting the influence of engine-nacelle volume and nacelle-wing interference lift on the flow field around the aircraft were inadequate and needed to be modified;

(4) conventional methods for integrating engine nacelles onto the wing/fuselage/fin(s) airframe need to be modified if the configuration is to generate low-boom pressure signatures on the ground during the supersonic-cruise segment of the mission;

(5) lift-measuring strain gauges need to be submerged below the surface of the sting so they do not generate shocks that encroach on the tail shock of the pressure signature.

References

1. Whitham, G. B.: *The Flow Pattern of a Supersonic Projectile.* Communications on Pure and Applied Mathematics vol. V, no. 3, August 1952, pp. 301-348.

2. Walkden, F.: *The Shock Pattern of a Wing-Body Combination, Far From the Flight Path.* Aeronautical Quarterly, vol. IX, pt. 2, May 1958, pp. 164-194. Society, vol. 65, no. 606, June 1961, pp. 433 - 436.

3. Jones, L. B.: *Lower Bounds For Sonic Bangs.* Journal of the Royal Aeronautical Society, vol. 65, no. 606, June 1961, pp. 433 - 436.

4. Seebass, R.; and George, A. R.: *Sonic-Boom Minimization.* Journal of the Acoustical Society of America, vol. 51, no. 2, pt. 3, February 1972, pp. 686 - 694.

5. Darden, Christine M.: *Sonic Boom Minimization With Nose-Bluntness Relaxation.* NASA TP-1348, 1979.

6. McLean, F. Edward: *Some Nonasymptotic Effects On the Sonic Boom of Large Airplanes.* NASA TN D-2877, 1965.

7. Carlson, Harry W.; Barger, Raymond L.; and Mack, Robert J.: *Application Of Sonic-Boom Minimization Concepts In Supersonic Transport Design.* NASA TN D-7218, June 1973.

8. Carlson, Harry W.: *An Investigation Of Some Aspects Of The Sonic Boom By Means Of Wind-Tunnel Measurements Of Pressures About Several Bodies At A Mach Number Of 2.01.* NASA TN D-161, December 1959.

9. Carlson, Harry W.: *An Investigation Of The Influence Of Lift On Sonic-Boom Intensity By Means Of Wind-Tunnel Measurements Of The Pressure Fields Of Several Wing-Body Combinations At A Mach Number Of 2.01.* NASA TN D-881, July 1961.

10. Morris, Odell A.: *A Wind-Tunnel Investigation At A Mach Number Of 2.01 Of The Sonic-Boom Characteristics Of Three Wing-Body Combinations Differing In Wing Longitudinal Location.* NASA TN D-1384, September 1962.

11. Carlson, Harry W.; and Shrout, Barrett L.: *Wind-Tunnel Investigation Of The Sonic-Boom Characteristics Of Three Proposed Supersonic Transport Configurations.* NASA TM X-889, October 1963.

12. Carlson, Harry W.; Mack, Robert J.; and Morris, Odell A.: *A Wind-Tunnel Investigation Of The Effect Of Body Shape On Sonic-Boom Pressure Distributions.* NASA TN D-3106, November 1965.

13. Carlson, Harry W.; McLean, F. Edward; and Shrout, Barrett L.: *A Wind-Tunnel Study Of Sonic-Boom Characteristics For Basic And Modified Models Of A Supersonic Transport Configuration.* NASA TM X-1236, May 1966.

14. Morris, Odell A.: *Wind-Tunnel Investigation Of Sonic-Boom Characteristics Of A Delta-Wing-Body Combination At Mach Numbers Of 1.41 And 2.01.* NASA TN D-3455, June 1966.

15. Morris, Odell A.; Lamb, Milton; and Carlson, Harry W.: *Sonic-Boom Characteristics In The Extreme Near Field Of A Complex Airplane Model At Mach Numbers Of 1.5, 1.8, And 2.5.* NASA TN D-5755, April 1970.

16. Shrout, Barrett L.; Mack, Robert J.; and Dollyhigh, Samuel M.: *A Wind-Tunnel Investigation Of Sonic-Boom Pressure Distributions Of Bodies Of Revolution At Mach 2.96, 3.83, and 4.63.* NASA TN D-6195, April 1971.

17. Miller, David S.; Morris, Odell A.; and Carlson, Harry W.: *Wind Tunnel Investigation Of Sonic-Boom Characteristics Of Two Simple Wing Models At Mach Numbers From 2.3 To 4.63*. NASA TN D-6201, April 1971.

18. Hunton, Lynn W.; Hicks, Raymond M.; and Mendoza, Joel P.: *Some Effects Of Wing Planform On Sonic Boom*. NASA TN D-7160, January 1973.

19. Mack, Robert J.; and Darden, Christine M.: *Wind-Tunnel Investigation Of The Validity Of A Sonic-Boom-Minimization Concept*. NASA TP-1421, 1979.

20. Carlson, Harry W.; and Mack, Robert J.: *Estimation Of Wing Nonlinear Aerodynamic Characteristics at Supersonic Speeds*. NASA TP-1718, 1980.

21. Mack, Robert J.; and Needleman, Kathy E.: *The Design Of Two Sonic Boom Wind Tunnel Models From Conceptual Aircraft Which Cruise At Mach Numbers Of 2.0 And 3.0*. AIAA-90-4026, AIAA 13th Aeroacoustics Conference, October 22-24, 1990.

22. Middleton, Wilbur D.; and Carlson, Harry W.: *A Numerical Method For Calculating Near-Field Sonic-Boom Pressure Signatures*. NASA TN D-3082, 1965.

23. Hayes, Wallace D.; Haefeli, Rudolph C.; and Kulsrud, H. E.: *Sonic Boom Propagation In A Stratified Atmosphere, With Computer Program*. NASA CR-1299, 1969.

24. Craidon, Charlotte B.: *Description Of A Digital Computer Program For Airplane Configuration Plots*. NASA TM X-2074, 1970.

Appendix A

Descriptions of the Mach 2 and the Mach 3 Low-Boom Concepts

The Mach 2 and Mach 3 concepts were designed to validate low-boom minimization, analysis, and design methodology that had been developed prior to the close of the SCAT and SCAR programs. They were to generate ground-level overpressures of about 1 psf while cruising at their respective design Mach numbers, beginning-cruise altitudes, and beginning-cruise weights. No attempts were made to size the concepts for enhanced mission performance or for optimized weights. The beginning-cruise weight, used to calculate sonic boom, was estimated from studies of previous high-technology concepts. Wing planform shapes, areas, spans, and dihedrals were selected primarily to match each concept's equivalent area distribution to their respective Seebass and George low-boom equivalent area distribution. Features that reduced both sonic boom and aerodynamic drag were kept; those that increased sonic-boom overpressures were bypassed even though they may have reduced the aerodynamic drag or the empty weight. Therefore, no gross take-off weights, empty weights, fuel weights, etc. are listed in the data below.

This design effort was to be the first of several steps to validate and, where necessary, update low-boom technology. Only after these methods had been fully validated, were they to be applied in concert with aerodynamic analysis, design, and optimization methods to configure a fully-integrated, mission-oriented, low-boom conceptual aircraft.

	Mach 2 Concept	Mach 3 Concept
Span, ft	160.0	144.0
Length, ft	313.0	330.0
Wing Lift Legth, ft	300.0	300.0
Wing Area, ft^2	15,055.0	16,605.0
Aspect Ratio, b^2/S	1.70	1.54
Cruise Altitude, ft	55,000.0	550,000.0
Beginning Cruise Weight, lb	550,000.0	550,000.0
Beginning Cruise Wing Loading, psf	36.5	33.1
Beginning Cruise C_L	0.06803	0.04421
Cruise Mach Number	2.0	3.0
Number of Engines	4	4
Ground-Level Overpressure, psf	1.0	1.0
Type of Low-Boom Signature Shape, reference 4	"Flat-Top:	"Ramp"

Appendix B

Numerical Description Of The Mach 2 Low-Boom Concept In Wave-Drag Format Of Reference 24; lengths in ft, areas in ft^2.

```
   1   1  -1   1   1   0   0 12 17   2 19 30 19   4              2 10   1 10
15054.8
0.0     2.5     5.0     10.0    15.0    20.0    30.0    40.0    50.0    60.0
70.0    80.0    85.0    90.0    95.0    97.5    100.0
16.0    6.0     -1.833  265.5
36.0    8.0     -3.084  246.0
76.0    12.0    -5.422  207.0
116.0   16.0    -7.544  168.0
156.0   20.0    -9.267  129.0
180.0   24.0    -9.991  106.0
204.0   29.0    -10.44  83.25
220.0   34.0    -10.51  68.5
232.0   39.0    -10.36  57.75
240.0   44.0    -10.08  51.0
280.0   76.0    -6.596  19.0
288.0   80.0    -6.208  12.0
0.0     .02133  -.0517  -.4270  -1.018  -1.717  -3.151  -4.584  -6.018  -7.452
-8.885  -10.32  -11.03  -11.61  -11.99  -12.10  -12.17
0.0     .03748  -.0138  -.3321  -.8533  -1.476  -2.755  -4.034  -5.314  -6.593
-7.872  -9.151  -9.791  -10.35  -10.73  -10.84  -10.92
0.0     .05224  .02976  -.1966  -.5938  -1.076  -2.070  -3.064  -4.057  -5.051
-6.044  -7.038  -7.535  -8.019  -8.376  -8.497  -8.578
0.0     .05180  .04480  -.1120  -.4032  -.7616  -1.501  -2.240  -2.979  -3.718
-4.458  -5.197  -5.566  -5.936  -6.258  -6.373  -6.456
0.0     .04132  .04031  -.0645  -.2661  -.5160  -1.032  -1.548  -2.064  -2.580
-3.096  -3.612  -3.870  -4.128  -4.381  -4.481  -4.558
0.0     .03056  .02981  -.0477  -.1968  -.3816  -.7632  -1.144  -1.526  -1.908
-2.290  -2.671  -2.862  -3.053  -3.244  -3.335  -3.409
0.0     .01517  .01054  -.0468  -.1495  -.2747  -.5328  -.7909  -1.049  -1.307
-1.565  -1.823  -1.952  -2.081  -2.210  -2.275  -2.339
0.0     .00070  -.0099  -.0582  -.1323  -.2192  -.3973  -.5754  -.7535  -.9316
-1.110  -1.288  -1.377  -1.466  -1.555  -1.599  -1.644
0.0     -.0113  -.0272  -.0707  -.1251  -.1848  -.3061  -.4273  -.5486  -.6699
-.7912  -.9124  -.9731  -1.034  -1.094  -1.125  -1.155
0.0     -.0204  -.0408  -.0816  -.1224  -.1632  -.2448  -.3264  -.4080  -.4896
-.5712  -.6528  -.6936  -.7344  -.7752  -.7956  -.8160
0.0     -.0076  -.0152  -.0304  -.0456  -.0608  -.0912  -.1216  -.1520  -.1824
-.2120  -.2432  -.2584  -.2736  -.2888  -.2964  -.0304
0.0     -.0048  -.0096  -.0192  -.0288  -.0384  -.0576  -.0768  -.0960  -.1152
-.1344  -.1536  -.1632  -.1728  -.1824  -.1872  -.1920
0.0     .10969  .21375  .405    .57375  .72     .945    1.08    1.125   1.08
.945    .72     .57375  .405    .21375  .10969  0.0
0.0     .10969  .21375  .405    .57375  .72     .945    1.08    1.125   1.08
.945    .72     .57375  .405    .21375  .10969  0.0
0.0     .10969  .21375  .405    .57375  .72     .945    1.08    1.125   1.08
.945    .72     .57375  .405    .21375  .10969  0.0
0.0     .10969  .21375  .405    .57375  .72     .945    1.08    1.125   1.08
.945    .72     .57375  .405    .21375  .10969  0.0
0.0     .10969  .21375  .405    .57375  .72     .945    1.08    1.125   1.08
.945    .72     .57375  .405    .21375  .10969  0.0
0.0     .10969  .21375  .405    .57375  .72     .945    1.08    1.125   1.08
.945    .72     .57375  .405    .21375  .10969  0.0
0.0     .11213  .2185   .414    .5865   .736    .966    1.104   1.15    1.104
```

```
.966     .736    .5865   .414    .2185   .11213 0.0
0.0      .11456  .22325  .423    .59925  .752    .987    1.128   1.175   1.128
.987     .752    .59925  .423    .22325  .11456 0.0
0.0      .1170   .228    .432    .612    .768    1.008   1.152   1.2     1.152
1.0080   .768    .612    .432    .228    .1170  0.0
0.0      .11944  .23275  .441    .62475  .784    1.029   1.176   1.225   1.176
1.029    .784    .62475  .441    .23275  .11944 0.0
0.0      .11944  .23275  .441    .62475  .784    1.029   1.176   1.225   1.176
1.0290   .784    .62475  .441    .23275  .11944 0.0
0.0      .11944  .23275  .441    .62475  .784    1.029   1.176   1.225   1.176
1.029    .784    .62475  .441    .23275  .11944 0.0
0.0      10.0    20.0    30.0    40.0    50.0    60.0    70.0    80.0    90.0
100.0    110.0   120.0   130.0   140.0   150.0   160.0   170.0   180.0   190.0
200.0    210.0   220.0   230.0   240.0   250.0   260.0   270.0   280.0   290.0
0.0      -.1008  -.3776  -.7921  -1.306  -1.881  -2.480  -3.080  -3.680  -4.280
-4.880   -5.480  -6.080  -6.680  -7.280  -7.880  -8.480  -9.080  -9.680  -10.28
-10.88   -11.48  -12.08  -12.66  -13.14  -13.52  -13.79  -13.95  -14.00  -13.95
0.0      7.5169  31.552  51.756  63.780  72.346  79.603  86.071  90.676  95.944
100.50   105.08  109.78  114.05  118.63  123.92  128.78  132.28  134.91  134.95
134.89   133.04  128.43  119.77  106.13  87.718  66.938  50.198  36.667  19.092
290.0    300.0   310.0   313.0
-13.95   -13.79  -13.52  -13.44
19.092   4.3458  .13377 0.0
260.0    12.0    -17.4
0.0      2.0     4.0     6.0     8.0     10.0    12.0    22.0    25.25   28.5
2.55     2.6111  2.6611  2.700   2.7278  2.7444  2.75    2.75    2.65    2.55
263.0    24.0    -16.8
0.0      2.0     4.0     6.0     8.0     10.0    12.0    22.0    25.25   28.5
2.55     2.6111  2.6611  2.700   2.7278  2.7444  2.75    2.75    2.65    2.55
230.0    0.0     -8.0    56.855  276.0   0.0     10.0    11.9
0.0      10.0    20.0    30.0    40.0    50.0    60.0    70.0    80.0    100.0
0.0      .45     .80     1.05    1.20    1.25    1.20    1.05    .80     0.0
```

Appendix C

Numerical Description of the Mach 3 Low-Boom Concept in Wave-Drag Format of Reference 24; lengths in ft, areas in ft^2.

```
   1   1  -1   1    1   0   0 13 17   2 19 20 19 19                    2 10   2 10
13450.1
0.0     2.5    5.0    10.0    15.0    20.0    30.0   40.0   50.0   60.0
70.0    75.0   80.0   85.0    90.0    95.0   100.0
54.4    7.2    -0.195 244.8
83.2    10.8   -1.489 216.0
112.0   14.4   -2.584 187.0
140.8   18.0   -3.333 158.4
169.6   21.6   -3.762 129.6
198.4   25.2   -4.059 101.7
227.2   28.8   -4.109 73.80
241.6   32.4   -3.974 60.3
248.8   36.0   -3.650 54.0
278.5   55.8   -1.065 29.25
287.0   60.65  -0.439 21.96
296.5   63.50  -0.100 13.175
310.0   64.8   -0.025 0.0
0.0     .02380 -.0238 -.2761 -.6426 -1.028 -1.799 -2.570 -3.342 -4.1126
-4.883 -5.270 -5.655 -6.041 -6.417 -6.699 -6.8666
0.0     .03720 .01140 -.1788 -.4698 -.7776 -1.393 -2.009 -2.624 -3.240
-3.856 -4.163 -4.471 -4.779 -5.087 -5.377 -5.573
0.0     .04037 .02808 -.0112 -.3370 -.5756 -1.053 -1.530 -2.008 -2.485
-2.963 -3.201 -3.440 -3.678 -3.917 -4.156 -4.3664
0.0     .03603 .03080 -.0704 -.2376 -.4158 -.7722 -1.129 -1.485 -1.841
-2.198 -2.376 -2.554 -2.732 -2.911 -3.089 -3.267
0.0     .02690 .02410 -.0468 -.1652 -.2916 -.5443 -.7970 -1.049 -1.3025
-1.555 -1.681 -1.808 -1.934 -2.061 -2.187 -2.313
0.0     .01590 .01271 -.0355 -.1144 -.1983 -.3661 -.5339 -.7017 -.8695
-1.038 -1.121 -1.205 -1.289 -1.373 -1.457 -1.541
0.0     .00540 .00082 -.0303 -.0775 -.1273 -.2269 -.3265 -.4262 -.5258
-.6254 -.6753 -.7250 -.7749 -.8248 -.8745 -.9243
0.0     -.0025 -.0094 -.0329 -.0633 -.0950 -.1583 -.2216 -.2849 -.3482
-.4116 -.4432 -.4748 -.5065 -.5382 -.5698 -.6015
0.0     -.0101 -.0203 -.0405 -.0608 -.0810 -.1215 -.1620 -.2025 -.2430
-.2835 -.3038 -.3240 -.3443 -.3645 -.3848 -.4050
0.0     -.0055 -.0110 -.0220 -.0329 -.0438 -.0658 -.0878 -.1097 -.1316
-.1535 -.1645 -.1755 -.1865 -.1975 -.2084 -.21938
0.0     -.0041 -.0080 -.0161 -.0241 -.0322 -.0482 -.0644 -.0805 -.09658
-.1127 -.1207 -.1288 -.1368 -.1449 -.1529 -.16096
0.0     -.0024 -.0050 -.0099 -.0148 -.0197 -.0296 -.0395 -.0493 -.05925
-.0691 -.0741 -.0790 -.0839 -.0888 -.0938 -.0984
0.0     0.0    0.0    0.0    0.0    0.0    0.0    0.0    0.0    0.0
0.0     0.0    0.0    0.0    0.0    0.0    0.0
0.0     .1219  .2375  .450   .6375  .80    1.05   1.20   1.250  1.20
1.05    .9375  .800   .6375  .450   .2375  0.0
0.0     .1158  .2256  .4275  .6052  .760   .9975  1.14   1.1875 1.14
.9975   .8904  .760   .6052  .4275  .2256  0.0
0.0     .1121  .218   .414   .5865  .736   .966   1.104  1.15   1.104
.966    .8625  .736   .5865  .414   .218   0.0
```

```
0.0     .1097   .2138   .405    .5738   .72     .945    1.08    1.125   1.08
.945    .8438   .72     .5738   .405    .2138   0.0
0.0     .1085   .2114   .4005   .5674   .712    .9345   1.068   1.1125  1.068
.9345   .8344   .7120   .5674   .4005   .2114   0.0
0.0     .1073   .2090   .396    .5610   .704    .924    1.056   1.100   1.056
.924    .825    .704    .561    .396    .209    0.0
0.0     .1097   .2138   .405    .5738   .72     .945    1.08    1.125   1.08
.945    .8438   .72     .5738   .405    .2138   0.0
0.0     .1048   .2043   .387    .5483   .688    .903    1.032   1.075   1.032
.903    .8063   .688    .5483   .38705  .2043   0.0
0.0     .1073   .1976   .3744   .5304   .6656   .8736   .9984   1.04    .9984
.8736   .78     .6656   .5304   .3744   .1976   0.0
0.0     .0975   .19     .36     .51     .64     .84     .96     1.0     .96
.84     .75     .64     .51     .36     .19     0.0
0.0     .0975   .19     .36     .51     .64     .84     .96     1.0     .96
.84     .75     .64     .51     .36     .19     0.0
0.0     .0975   .19     .36     .51     .64     .84     .96     1.0     .96
.84     .75     .64     .51     .36     .19     0.0
0.0     .0975   .19     .36     .51     .64     .84     .96     1.0     .96
.84     .75     .64     .51     .36     .19     0.0
0.0     3.0     6.0     9.0     12.0    15.0    20.0    30.0    40.0    50.0
60.0    70.0    80.0    90.0    100.0   110.0   120.0   130.0   140.0   150.0
0.0     .10     .20     .30     .40     .50     .70     1.05    1.20    1.15
.875    .550    .225    -.10    -.45    -.775   -1.1    -1.425  -1.750  -2.075
0.0     .18095  1.0207  2.7172  5.4739  9.5115  20.428  78.540  131.51  153.94
164.67  169.25  171.57  171.10  170.64  167.87  163.77  158.81  152.18  145.91
150.0   160.0   170.0   180.0   190.0   200.0   210.0   220.0   230.0   240.0
250.0   260.0   270.0   280.0   290.0   300.0   310.0   320.0   330.0
-2.075  -2.40   -2.75   -3.05   -3.40   -3.725  -4.05   -4.375  -4.70   -5.05
-5.30   -5.475  -5.55   -5.55   -5.55   -5.55   -5.55   -5.55   -5.55
145.91  139.77  134.16  128.68  124.69  120.76  118.44  117.67  120.37  125.88
136.02  141.03  133.96  115.37  87.583  55.947  28.653  8.1433  0.0
277.0   10.8    -10.752
0.0     2.0     4.0     6.0     8.0     10.0    12.0    22.0    28.0    30.5
2.55    2.6111  2.6611  2.70    2.7278  2.7444  2.75    2.75    2.75    2.75
277.0   18.0    -10.195
0.0     2.0     4.0     6.0     8.0     10.0    12.0    22.0    28.0    30.5
2.55    2.6111  2.6611  2.70    2.7278  2.7444  2.75    2.75    2.75    2.75
257.0   0.0     1.18    59.314  297.0   0.0     15.449  21.0
0.0     10.0    20.0    30.0    40.0    50.0    60.0    70.0    80.0    100.0
0.0     .45     .80     1.05    1.20    1.25    1.20    1.05    .80     0.0
257.0   0.0     1.18    59.314  316.0   0.0     -3.55   0.0
0.0     10.0    20.0    30.0    40.0    50.0    60.0    70.0    80.0    100.0
0.0     .45     .80     1.05    1.20    1.25    1.20    1.05    .80     0.0
```

REPORT DOCUMENTATION PAGE		*Form Approved* *OMB No. 0704-0188*

The public reporting burden for this collection of information is estimated to average 1 hour per response, including the time for reviewing instructions, searching existing data sources, gathering and maintaining the data needed, and completing and reviewing the collection of information. Send comments regarding this burden estimate or any other aspect of this collection of information, including suggestions for reducing this burden, to Department of Defense, Washington Headquarters Services, Directorate for Information Operations and Reports (0704-0188), 1215 Jefferson Davis Highway, Suite 1204, Arlington, VA 22202-4302. Respondents should be aware that notwithstanding any other provision of law, no person shall be subject to any penalty for failing to comply with a collection of information if it does not display a currently valid OMB control number.
PLEASE DO NOT RETURN YOUR FORM TO THE ABOVE ADDRESS.

1. REPORT DATE *(DD-MM-YYYY)* 01- 10 - 2003	2. REPORT TYPE Technical Memorandum	3. DATES COVERED *(From - To)*
4. TITLE AND SUBTITLE An Analysis of Measured Pressure Signatures From Two Theory-Validation Low-Boom Models		**5a. CONTRACT NUMBER**
		5b. GRANT NUMBER
		5c. PROGRAM ELEMENT NUMBER
6. AUTHOR(S) Mack, Robert J.		**5d. PROJECT NUMBER**
		5e. TASK NUMBER
		5f. WORK UNIT NUMBER 23-706-92-02
7. PERFORMING ORGANIZATION NAME(S) AND ADDRESS(ES) NASA Langley Research Center Hampton, VA 23681-2199		**8. PERFORMING ORGANIZATION REPORT NUMBER** L-18318
9. SPONSORING/MONITORING AGENCY NAME(S) AND ADDRESS(ES) National Aeronautics and Space Administration Washington, DC 20546-0001		**10. SPONSOR/MONITOR'S ACRONYM(S)** NASA
		11. SPONSOR/MONITOR'S REPORT NUMBER(S) NASA/TM-2003-212423

12. DISTRIBUTION/AVAILABILITY STATEMENT
Unclassified - Unlimited
Subject Category 05
Availability: NASA CASI (301) 621-0390   Distribution: Nonstandard

13. SUPPLEMENTARY NOTES
An electronic version can be found at http://techreports.larc.nasa.gov/ltrs/ or http://ntrs.nasa.gov

14. ABSTRACT
Two wing/fuselage/nacelle/fin concepts were designed to check the validity and the applicability of sonic-boom minimization theory, sonic-boom analysis methods, and low-boom design methodology in use at the end of the 1980ís. Models of these concepts were built, and the pressure signatures they generated were measured in the wind-tunnel. The results of these measurements lead to three conclusions: (1) the existing methods could adequately predict sonic-boom characteristics of wing/fuselage/fin(s) configurations if the equivalent area distributions of each component were smooth and continuous; (2) these methods needed revision so the engine-nacelle volume and the nacelle-wing interference lift disturbances could be accurately predicted; and (3) current nacelle-configuration integration methods had to be updated. With these changes in place, the existing sonic-boom analysis and minimization methods could be effectively applied to supersonic-cruise concepts for acceptable/tolerable sonic-boom overpressures during cruise.

15. SUBJECT TERMS
Sonic boom; Whitham theory; Minimization theory; Wind-tunnel models

16. SECURITY CLASSIFICATION OF:			17. LIMITATION OF ABSTRACT	18. NUMBER OF PAGES	19a. NAME OF RESPONSIBLE PERSON STI Help Desk (email: help@sti.nasa.gov)
a. REPORT	b. ABSTRACT	c. THIS PAGE			19b. TELEPHONE NUMBER *(Include area code)*
U	U	U	UU	24	(301) 621-0390